Gene expression analysis of bovine embryonic disc, trophoblast and parietal hypoblast at the start of gastrulation

Peter L. Pfeffer[1,2], *Craig S. Smith*[2,3], *Paul Maclean*[2] *and Debra K. Berg*[2]

School of Biological Science, Victoria University of Wellington, Wellington, New Zealand; Agresearch, Ruakura Campus, 1 Bisley Street, Hamilton, New Zealand; and School of Medicine, University of Notre Dame Australia, Sydney, Australia

Summary

In cattle early gastrulation-stage embryos (Stage 5), four tissues can be discerned: (i) the top layer of the embryonic disc consisting of embryonic ectoderm (EmE); (ii) the bottom layer of the disc consisting of mesoderm, endoderm and visceral hypoblast (MEH); (iii) the trophoblast (TB); and (iv) the parietal hypoblast. We performed microsurgery followed by RNA-seq to analyse the transcriptome of these four tissues as well as a developmentally earlier pre-gastrulation embryonic disc. The cattle EmE transcriptome was similar at Stages 4 and 5, characterised by the OCT4/SOX2/NANOG pluripotency network. Expression of genes associated with primordial germ cells suggest their presence in the EmE tissue at these stages. Anterior visceral hypoblast genes were transcribed in the Stage 4 disc, but no longer by Stage 5. The Stage 5 MEH layer was equally similar to mouse embryonic and extraembryonic visceral endoderm. Our data suggest that the first mesoderm to invaginate in cattle embryos is fated to become extraembryonic. TGFβ, FGF, VEGF, PDGFA, IGF2, IHH and WNT signals and receptors were expressed, however the representative members of the FGF families differed from that seen in equivalent tissues of mouse embryos. The TB transcriptome was unique and differed significantly from that of mice. FGF signalling in the TB may be autocrine with both FGFR2 and FGF2 expressed. Our data revealed a range of potential inter-tissue interactions, highlighted significant differences in early development between mice and cattle and yielded insight into the developmental events occurring at the start of gastrulation.

Keywords: Cattle, Embryo, Gastrulation, Preimplantation, RNA-seq

Introduction

Understanding the first 2 weeks of cattle embryonic development is of scientific as well as commercial relevance as during this period the greatest rate of conceptus loss is seen (Ayalon, 1978; Sartori *et al.*, 2010; Diskin *et al.*, 2011). The problem is equally apparent in embryo transfer experiments. Growing embryos in culture to the blastocyst stage and then transferring into recipients revealed losses of 24% in the second week of development (Berg *et al.*, 2010).

Such losses may not be surprising, considering the critical developmental events that occur during this week (Pfeffer, 2014; van Leeuwen *et al.*, 2015). At the end of the first week, the successful embryo has undergone the first lineage specification event resulting in two distinct lineages, namely the inner cell mass (ICM) and the outer trophectoderm. The trophectoderm becomes committed to the trophoblast fate during the second week (Berg *et al.*, 2011), then gradually starts to form a subpopulation (20%) of interspersed terminally differentiated binucleate cells (Wooding, 1992). Towards the end of the second week, the trophoblast overlying the epiblast (termed Rauber's layer or polar trophoblast) has disappeared, exposing the outer surface of the ICM/epiblast to the maternal environment (van Leeuwen *et al.*, 2015).

---

[1]All correspondence to: P.L. Pfeffer. School of Biological Science, Victoria University of Wellington, Wellington, New Zealand. Tel: +64 4 4637462. Fax: +64 4 4635331. E-mail: peter.pfeffer@vuw.ac.nz
[2]Agresearch, Ruakura Campus, 1 Bisley Street, Hamilton, New Zealand.
[3]School of Medicine, University of Notre Dame Australia, Sydney, Australia.

The inner cell mass forms two layers by embryonic day 9 (day 0 corresponds to fertilization), namely the epiblast and underlying hypoblast (Maddox-Hyttel *et al.*, 2003). The hypoblast (also termed primitive endoderm) migrates to line the entire blastocyst cavity thus underlying both the epiblast and the trophoblast. The hypoblast under the epiblast is now at Stage 2, (see van Leeuwen *et al.*, 2015, for staging used here) termed the visceral hypoblast, whereas that underlying the 'mural' trophoblast is the 'parietal' hypoblast (mural and parietal are derived from Latin: 'belonging to walls' to indicate their structurally supportive function for the embryo proper). From approximately 12 days after fertilization (Stage 3), one end of the visceral hypoblast changes morphology, becoming thicker, with projections to the epiblast. This thickened area is termed the anterior visceral hypoblast (AVH) and is presumed to be homologous to the anterior visceral endoderm (AVE) of the mouse and the anterior marginal crescent of the rabbit by virtue of expressing NODAL signalling inhibitors (van Leeuwen *et al.*, 2015). The mouse AVE has been shown to direct gastrulation (which requires NODAL) to the opposite end of the epiblast (Lu *et al.*, 2001).

After the overlying trophoblast has disappeared, the epiblast − during Stage 4 − transitions into a one- to two-cell layered epithelium, known as the embryonic ectoderm (EmE). By Stage 5, cells accumulate at the posterior margin of the EmE and then will translocate in a medial anterior direction, forming a groove (the primitive streak) with the funnel-shaped node at its anterior end. Some cells at the posterior margin and along the primitive streak and node will undergo an epithelial−mesenchymal transition and migrate out of the plane of the EmE. Endoderm cells will integrate into the underlying visceral hypoblast layer, displacing these cells in an anterior direction. Mesoderm cells will populate the space between the EmE and hypoblast/endoderm. Mesoderm cells migrating beyond the borders of the EmE will come to line the trophoblast and parietal hypoblast and thus form extraembryonic mesoderm. Mesoderm cells underlying the EmE form the (embryonic) mesoderm layer. At this stage AVH markers are no longer detectable (van Leeuwen *et al.*, 2015). The epiblast or EmE and underlying layers are easily identifiable by dissecting microscope and are collectively termed the embryonic disc.

While we have recently described the morphology of, and expression of, select genes in the various tissues seen at these embryonic stages (van Leeuwen *et al.*, 2015), little information is known about the global transcriptome at the tissue level. Whole embryo gene expression profiling has been reported (Mamo *et al.*, 2011), however such studies would predominantly capture the trophoblast tissue as the parietal hypoblast

to trophoblast cell ratio is only about 1 to 10 and the embryonic disc represents an even smaller part of the whole conceptus during this period. We have here exploited the power and accuracy of RNA-seq combined with an isothermal amplification procedure to allow us to capture the gene expression profile of all four separable tissues of a single cattle early gastrulation (Stage 5) embryo. To allow a better developmental understanding of the complex embryonic disc tissue, we additionally included the analysis of a Stage 4 disc.

Materials and Methods

Embryo collection and dissection

All animal work was approved by the Ruakura Animal Ethics committee RAEC 12025 (Hamilton, New Zealand) and all efforts were made to minimize suffering. *In vitro* produced embryos were generated as previously described (Berg *et al.*, 2010), using oocytes from uncharacterised dairy cows and sperm from a Friesian bull. On day 7 following IVF, Grade 1 and Grade 2 blastocysts were transferred to recipient animals and recovered on day 14 or 15 after fertilization, as previously described in detail (van Leeuwen *et al.*, 2015). Reagents were from Sigma if not indicated otherwise. After collection in ePBS (enriched phosphate-buffered medium: Ca-/Mg-free PBS tablets with 0.0132 g/l $CaCl_2.2H_2O$, 0.010 g/l $MgCl_2.6H_2O$, 0.036 g/l sodium pyruvate, 1 g/l glucose, penicillin/streptomycin and 10% FCS), embryos were split into TB and embryonic disc-containing parts, then washed three times for 5 min in DMEM. The embryonic disc was cut away from surrounding tissue using microknives (Ultra Sharpe Splitting Blades, Bioniche Animal Health Asia, Australia), then digested for 3 min on ice with pancreatin/trypsin (2.5% w/v pancreatin; 0.5% trypsin; 0.5% polyvinylpyrrolidone) in Ca-/Mg-free Tyrodes−Ringers saline (per litre 8.0 g NaCl, 0.30 g KCl, 0.093 g $NaH_2PO_4.5H_2O$, 0.025 g KH_2PO_4, 1.0 g $NaHCO_3$, 2.0 g glucose). The disc was transferred to cold DMEM with 10% FCS and the underlying endoderm/mesoderm/visceral hypoblast layer carefully peeled off the embryonic ectoderm using watchmaker's tweezers (Dumont #5 biologie, ProSciTech, Australia). Both tissues were rinsed in cold PBS before transferral in 1 μl volume to 0.6 ml microcentrifuge tubes and freezing in liquid nitrogen before storage at −80°C. TB and parietal hypoblast required a 5 to 6 min enzymatic digestion period. For this work, all four tissues, from a single day 15 embryo, were used for RNA sequencing. Additionally a whole embryonic disc from a day 14 embryo was analysed. At that developmental stage we were unable to cleanly

Table 1 Embryo characteristics

Sample	Age (days)	Embryo length (mm)	ED length, width (μm)
Stage 4 (EmE stage)	14	1.3	200; 190
Stage 5 EG (early gastrula)	14	35	650; 440

separate the embryonic ectoderm and underlying visceral hypoblast. Physical characteristics of these two embryos are shown in Table 1.

RNA sequencing

RNA was isolated using Trizol, followed by DNase I digestion and ethanol precipitation as previously described (Smith *et al.*, 2007). RNA was amplified by isothermal strand displacement using the Ovation RNA-seq V2 system (NuGEN; Millennium Science, Wellington, NZ), which enriches for poly-A-containing mRNA. Yields of amplified cDNA were between 6.6 and 11 μg. Amplified DNA was sent to Macrogen (Seoul, Korea) for Illumina library construction (RNA TruSeq) and sequencing (Illumina HiSeq2000). Both ends of fragments (average length between 441 and 501 bp) at a sequencing depth of 46 to 74 million per sample (Table 2). Illumina 1.9 encoding indicated excellent sequencing quality (scores >28) of reads up to 100 bp. Regions of low quality sequence and Illumina primers and adapters remaining from the sequencing process were removed from the reads using Flexbar (Dodt *et al.*, 2012). The trimmed reads were then mapped against the *Bos taurus* UMD3.1 genome using TopHat software (Trapnell *et al.*, 2009), and against the NCBI *Bos taurus* RefSeq mRNA using BWA (Li & Durbin, 2009). The percentages mapped are shown in Table 1. Reads mapping to the RefSeq database were normalised for transcript length (FPK, Fragment reads Per Kilobase of exon) then adjusted using negative binomial modelling and the edgeR program (Robinson *et al.*, 2010) within R (R Core Team, 2014). Total numbers of adjusted FPK for the five samples ranged from 8.3 to 8.6 million and were converted to FPKM (FPK per million reads). The data are available as Supporting Information (Table S1).

Data analysis

An FPKM of one for a RefSeq (NCBI) transcript (subsequently referred to as 'gene') corresponds to approximately one mRNA molecule per cell (Mortazavi *et al.*, 2008). Samples exhibiting an FPKM for a gene of less than one were set to equal 1 ('cut-off'). Genes for which FPKM = 1 for all five samples were ignored. All analyses were done on log (base two) transformed values. For differential expression analyses, expression levels were classified into 10 log base 2 'bins' (0 to 11), with bin 'x' containing values

where $x \leq \log_2 (FPKM) < (x + 1)$ for $x = 1$ to 10. For bin 11 ($x = 11$), x was $\leq \log_2 (FPKM)$, with no upper limit, to capture all highly expressed genes. Binary patterns were derived following the concept of Yanai *et al.* (2005). For this calculation, a 'gap' index was assigned to each gene by sorting the bin values of the five samples and determining the maximum difference ('gap') between neighbouring values. For profiles with a gap of at least 3 (corresponding to a greater than four-fold difference in expression), expression above the gap was classified as over-expressed (= 1), below as under-expressed (0) (Yanai *et al.*, 2005). Where two gaps were found for one gene, the lower bin value was used. Where no gap was found, expression was set to 1 (expressed) for all samples with an FPKM value above the cut-off. The binary expression values for each gene were assembled into a five digit pattern, e.g. DEMHT = 01010 means that this gene in: Stage 4 embryonic disc (= D) is not expressed, EmE (= E) is expressed, MEH (= M) is not expressed, PH (= H) is expressed and TB (= T) is not expressed. The binary codes were used to exclude 'common' genes expressed in all (code 11111) or all-but-one samples (01111, 10111, 11011, 11101, 11110), and for generating (using Microsoft Excel) the data in the Venn diagram (Fig. 1E). The Venn diagram was populated manually using a graphics program (Adobe Illustrator). The principal component analysis was generated using the pca.srbct function in R (R Core Team, 2014), using all genes for which expression was evident in at least one sample. Our gene expression data and assembled lists of genes (genes associated with mouse embryonic stages and tissues; genes expressed in cattle blastocyst lineages) were uploaded and analysed via the Ingenuity Core program (Qiagen, Dusseldorf, Germany). For creating the cattle blastocyst lists, the published gene sets (Nagatomo *et al.*, 2013; Ozawa *et al.*, 2012) for each lineage (ICM and TE) were compared and genes expressed in both datasets were used. *P*-values for analyses of Pathways, Biological functions and curated gene list comparisons were calculated within Ingenuity using the right-tailed Fisher's Exact Test.

Results

Sample characteristics and gene expression

Four tissue types were analysed from an embryo, which was generated by *in vitro* embryo production,
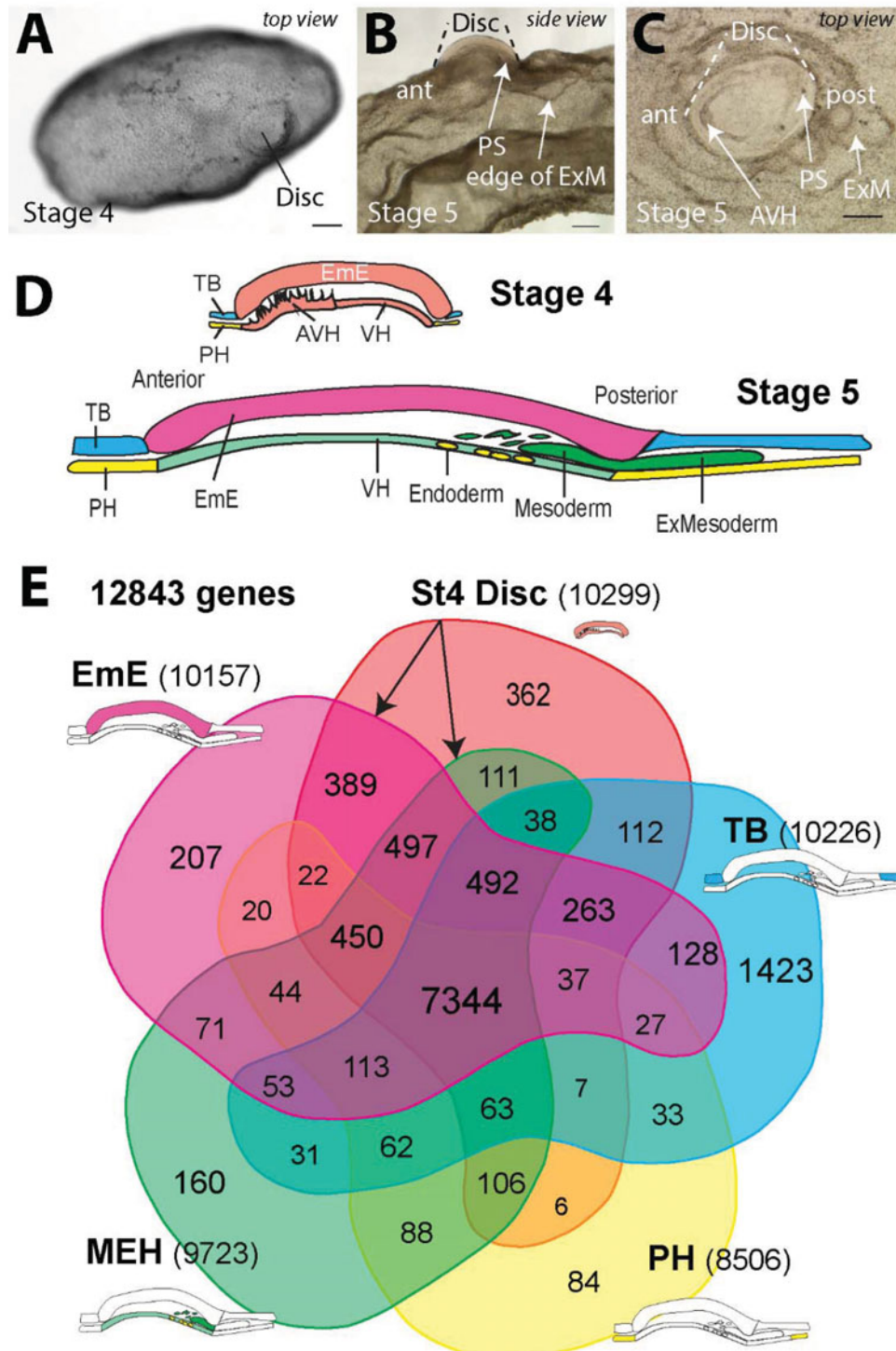
Figure 1 Differential expression of genes. (*A−C*) Features of Stage 4 and Stage 5 embryos as seen before dissection. Scale bars are 200 µm. (*D*) Embryonic regions are graphically depicted (cross-section through embryo, colour coded) with nomenclature as previously defined (van Leeuwen *et al.*, 2015). (*E*) Venn diagrams of differentially expressed genes with insets showing origin of tissues. Arrows indicate that EmE and MEH are descendant tissues of Stage 4 embryonic disc. AVH, anterior visceral hypoblast; disc, embryonic disc; E, endoderm; EmE, embryonic ectoderm; ExM, extraembryonic mesoderm; PH, parietal hypoblast; PS, primitive streak region; TB, trophoblast; VH, visceral hypoblast.

Table 2 Overview of RNA-seq results

Sample	Average size (bp)	Number of fragments	% RefSeq[a]	% non-RefSeq[b]	% mapped
Stage 4: Disc	481	47,681,017	28	42	70
Stage 5: EmE	479	68,490,193	25	51	75
Stage 5: MEH	447	74,522,098	29	52	81
Stage 5: PH	501	46,483,443	25	51	76
Stage 5: TB	441	66,016,989	12	65	77

[a]Percentage uniquely mapped to RefSeq database (NCBI) RNA sequences.
[b]Number of fragments (excluding those already mapped to RefSeq) uniquely mapped to *Bos taurus* UMD3.1 genome.
Disc, embryonic disc; EmE, embryonic ectoderm; MEH, mesoderm, endoderm and visceral hypoblast; PH, parietal hypoblast; TB, trophoblast.

then transferred as an expanded blastocyst into a synchronised recipient cow and retrieved 14 days after fertilization. Using embryo size and epiblast size (Table 1 and Fig. 1), the embryo was classified as Stage 5, early gastrulation (van Leeuwen *et al.*, 2015). The four tissues included the upper layer of the embryonic disc, which is composed of the embryonic ectoderm (EmE), wherein the primitive streak and node form; the cells underlying the embryonic ectoderm composed of a mixture of visceral hypoblast cells, endoderm and mesoderm (MEH); parietal hypoblast (PH) and trophoblast (TB).

PH and TB were taken well away from the embryonic disc to remove the possibility of contamination with extraembryonic mesoderm, which at this stage migrates out from the edges of the embryonic disc in-between the TB and PH and was evident under the dissecting microscope (Fig. 1*B*, *C*). The position of these tissues are indicated (Fig. 1*D*, *E*). Lastly, an embryonic disc of a Stage 4 embryo was analysed (Table 1 and Fig. 1*A*). In total, 50 million to 70 million reads were obtained for each tissue. Mapping revealed that a quarter of reads could be assigned to known reference sequences, except for the TB tissue, for which only an eighth could be assigned. The overall fraction of sequence that could be matched to the bovine genome was between 70 and 81% (Table 2). It is unclear whether the lower reference sequence recognition rate for the TB tissue is caused by an experimental artefact such as increased DNA contamination in the RNA preparation or has a biological reason such as differential splicing or increased transcription of non-reference genes.

In total, 12,843 genes were found to be expressed. For analysing differential expression among the figures tissues we used an algorithm that incorporated relative expression levels in addition to a more simple lower threshold level (Yanai *et al.*, 2005). Thus greater than four- to eight-fold jumps (or 'gaps', see Materials and methods) in expression levels were also considered in scoring expression, with only tissues above this gap scored as over-expressing a gene. Using

this scheme and representing the results in a five-fold Venn diagram (Fig. 1*E*), revealed the following:

- The early disc has more uniquely expressed genes (362) than either of its descendant tissues (EmE, 207; MEH, 160).
- The Stage 5 EmE is much more closely related to the Stage 4 embryonic disc than is the Stage 5 MEH tissue (389 versus 111).
- The parietal hypoblast is most closely related to the MEH tissue.
- The trophoblast shows the most divergent gene expression profile with a large number of genes (14% of TB genes) uniquely expressed. The other tissues only contain 1 to 4% unique genes.

We further compared the relatedness of the five tissues using principal component analysis without scoring for differential expression (Fig. 2). This comparison again revealed the close relationship of the Stage 5 EmE to the Stage 4 disc, a greater divergence of the MEH and the large divergence of the Stage 5 PH and TB tissues form the early disc. Notably the Stage 5 parietal hypoblast is most similar to the MEH (mesendoderm and visceral hypoblast) presumably as both share hypoblast-derived tissue.

Comparison of bovine to mouse embryonic gene expression profiles

We next asked how similar the tissues that we isolated were to mouse embryonic tissues. Lists of genes expressed in particular embryonic tissues and cells were compiled based on published whole mount *in situ* expression patterns from embryonic day 5.5 to 8 pre- to post-gastrulation mouse embryos (Table 3).

Only genes represented in four or less of the 12 mouse tissues were used. These lists were compared with our bovine tissue lists compiled by excluding common genes (expressed in more than three of the five samples) and including, for each tissue, only the genes scored as (over-)expressed according to our algorithm. As whole mount *in situ* hybridization is not

**Table 3** List of mouse gene sets and domains they are expressed in

Epiblast/EmE (30)	ACVR1B, CNRIP1, EOMES, ESRRB, EVX1, FGF4, FGF5, FGFR1, FOXH1, GDF3, HESX1, IFITM1, IGFBP3, IHH, LPAR4, NANOG, NODAL, OTX2, POU5F1, RARG, SOX2, T, TDGF1, WNT3
PGC, Primordial germ cells (22)	ALPL, CBX7, DAZ2, DDX4, DND1, Dppa3, FUT4, IFITM1, IFITM2, IFITM3, KDM4B, KLF2, LRRN3, NANOG, NANOS3, POU5F1, PRDM1, PRDM14, Rhox6/Rhox9, SMAD5, SOX2, TFAP2C
Node and primitive streak (89)	ARG1, ATP9A, BICC1, BMP7, C15orf65, C4orf22, CA3, CALCA, CDO1, CDX1, CELSR1, CFAP126, CFC1/CFC1B, CHRD, CYB561, DACT1, Defa-rs2, DMGDH, EOMES, EVX1, FABP7, Fam183b, FGF3, FGF4, FGF8, FOXD4L1, FST, FURIN, GAL, GBX1, GBX2, GSC, GSN, GSTM3, HDC, HES1, HOXB1, HOXB2, HOXB8, JOSD2, KDR, LEF1, LEFTY2, LHX1, LYPD6B, MESP1, MGST1, MLF1, MMP15, MNX1, NKX1–2, NODAL, NOG, NOTCH1, NOTCH2, PIM1, PKD1L1, PLET1, PRDM1, PRNP, REC8, RIPK3, RSPO3, SALL3, SCARA3, SEL1L3, SHH, SMIM22, SMOC1, SNAI1, SPRY1, SPRY2, T, TBX6, TDGF1, TGM2, TLX2, TMEM176A, TMEM176B, TRH, UPK3A, VTN, WNT3, WNT11, WNT2B, WNT5A, WNT8A, ZIC2, ZIC3
Endoderm, definitive (32)	ADCY8, AIM1, BMP2, CER1, CITED2, CLDN4, CLU, CPM, CPN1, DDO, DMGDH, EFNA1, GBX2, GPX2, GRIK3, GSC, GSN, HESX1, HHEX, IGFBP3, ISM1, ITGA3, LEFTY1, LPAR3, PPP1R14A, PRDM1, SEL1L3, SOX17, TMEM176A, TMEM176B, VTN, ZIC3
Extraembryonic mesoderm (15)	BMP2, BMP4, BMP7, CDX2, FGF8, HOXA3, HOXC8, KDR, LMO2, SALL3, SMAD2, SMAD5, T, WNT11, WNT5A
Mesoderm, embryonic, days 6.5–8, (42)	ALDH1A2, BMP5, BMP7, CDX1, CFC1/CFC1B, CHRD, CITED1, CITED2, CYP26A1, DLL1, DNAI1, EOMES, EPHA4, FGF4, FGF8, FOXC1, FOXD4, FST, GBX1, GBX2, HOXA1, HOXA3, HOXB1, HOXB2, HOXB8, JAG1, LEFTY2, MEIS1, MEOX1, MESP1, MYL1, NOG, NOTCH1, PCSK5, SMOC1, T, TDGF1, TLE3, TLE4, TLX2, WNT3, WNT5A
AVH/AVE, anterior visceral endoderm (14)	AMOT, CER1, CITED2, DKK1, GSC, HESX1, HHEX, LEFTY2, LHX1, NODAL, OTX2, SFRP1, SFRP5, SOX17
VH, visceral hypoblast/primitive endoderm (27)	AFP, AMN, BMP2, CDX1, CER1, CITED1, FGF8, FURIN, GATA4, GATA6, GSC, HESX1, HHEX, HNF1B, HNF4A, IHH, LEFTY1, NODAL, Otx2, OTX2, PLAU, PTH1R, SERPINB5, SFRP5, TF, TTR, VIL1
ExVH, extraembryonic visceral hypoblast/primitive endoderm (21)	ACVR1, AFP, AMN, APOE, BMP2, BMP4, CITED1, CYP26A1, FURIN, GATA4, GJA1, HAND1, HNF1B, HNF4A, IHH, SERPINB5, SOX17, TF, TGM2, TTR, VIL1
PH, parietal hypoblast (21)	CITED1, CYP26A1, FST, HNF1B, KRT19, LAMA1, LAMB1, PDGFA, PDGFRA, PDGFRB, PLAT, PTH1R, SEL1L3, SNAI1, SOX7, SOX17, SPARC, TF, THBD, TMPRSS2, VIM
ExE, extraembryonic ectoderm (25)	ACVR1B, ACVR2B, ATP9A, BMP4, CDX2, DLL1, ELF5, EOMES, ERF, ESRRB, ETS2, FGFR2, FOXD3, FRS2, FURIN, KDR, PCSK6, POU2F1, REEP5, SMAD3, SMARCA4, SOX2, TEAD4, TFAP2C, ZIC2
EPC, ectoplacental cone (20)	ASCL2, ATP9A, DLX3, ETS2, FLT1, GCM1, HAND1, ID2, INHBB, MMP9, NR6A1, PLAC8, POU2F1, RAN, REEP5, SCT, SNAI1, STRA13, TFAP2C, TPBPA

as sensitive as RNA-seq, a higher cut-off of FPKM = 2 was used. The significance of the overlaps between the bovine and mouse lists is shown in Fig. 3.

Key observations are:

- Stage 4 Embryonic disc is most similar to mouse epiblast/embryonic ectoderm tissue, anterior visceral endoderm (hypoblast) and primordial germ cells.
- Stage 5 EmE tissue closely resembles the mouse EmE tissue and also matches mouse primordial germ cell gene markers.

- MEH tissue is heterogeneous in its gene expression profile matches. On the one hand, the nascent endomesodermal cells reflect their embryonic ectodermal origin, and show highly significant matches to mouse primitive streak and node markers, definitive endoderm and extraembryonic mesoderm. Of note, no similarity to embryonic mesoderm is seen at this stage. On the other hand, the hypoblast component of the MEH expression profile matches mouse visceral as well as extraembryonic visceral endoderm/hypoblast. The tissue exhibits weaker
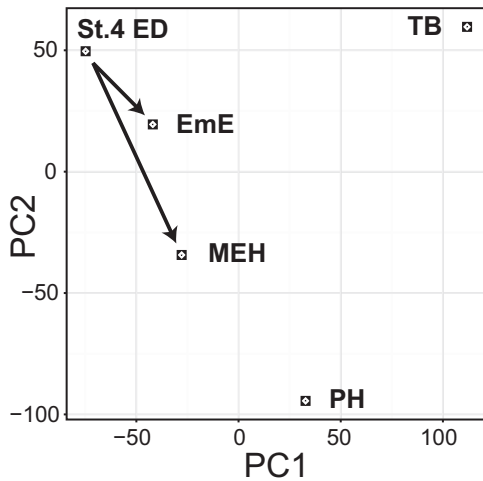
Figure 2 Principal component analysis of gene expression. Arrows indicate developmental resolution of Stage 4 embryonic disc into the Stage 5 derivatives of embryonic ectoderm and underlying visceral hypoblast/mesendoderm. Principal component variable 1 (PC1) explained 42% of the variation, PC2 32%. ED, embryonic disc; EmE, embryonic ectoderm; MEH, mesoderm, endoderm, visceral hypoblast; PH, parietal hypoblast; TB, trophoblast.

	Disc	EmE	MEH	PH	TB
Epiblast derived					
Epiblast/EmE	10.5	11.6	5.7		
PGC formation	4.9	3.4	0.7		0.3
Streak/Node	2.4	2.6	4.7	1.4	
Endoderm	3.6	0.5	3.3	1.9	
Mesoderm-Ex		1.3	1.6	0.7	
Mesoderm-Em		0.6	0.5		
Hypoblast derived					
AVH (AVE)	5.1	1.4	2.7		
VH	3.6	0.7	5.9	2.1	
ExVH	2.6		5.7	2.4	
PH	1.9	1.5	2.7	0.6	
Trophoblast derived					
ExE	1.1	2.0	1.0		0.2
EPC	2.2	1.7	0.2		1.6
Cattle blastocyst					
ICM	10.4	6.3	9.8	5.2	
TE	0.7	0.8			2.0

Figure 3 Comparison to marker genes. For each tissue all genes differentially expressed above a FPKM cut-off of 2 but excluding those common to at least four of the five tissues, were compared to curated sets of mouse tissue-specific genes (Table 3), listing the −log(P-value) of the dataset overlaps. Shading indicates the significance levels visually: black, P < 0.001; dark grey, P < 0.01; light grey, P < 0.05 (e.g. 1.3 = −log(0.05)). AVE, anterior visceral primitive endoderm; EPC, ectoplacental cone (mouse); Em, embryonic; Ex, extraembryonic; ExE, extraembryonic ectoderm; PGC, primordial germ cells; PH, parietal endoderm/hypoblast; VH, visceral endoderm/hypoblast.

Canonical Pathway	Disc	EmE	MEH	PH	TB
Wnt/β-catenin Signaling	4.3	4.7	3.9	2.4	0.0
PCP pathway	3.7	3.0	4.9	0.6	0.0
Human Embryonic Stem (ES) Cell Pluripotency	4.6	4.0	6.1	0.8	0.9
Transcriptional Regulatory Network in ES Cells	3.7	3.4	2.2	1.7	1.1
ES Cell Differentiation into Cardiac Lineages	3.6	3.9	1.2	0.9	0.3
Factors Promoting Cardiogenesis in Vertebrates	1.7	1.4	3.8	2.6	0.8
Cardiomyocyte Differentiation via BMP Receptors	0.8	0.5	2.9	2.5	0.0
Glutathione Redox Reactions I	1.3	1.4	3.6	2.4	0.4
PAK Signaling	0.6	0.0	0.6	2.4	0.6
Actin Cytoskeleton Signaling	0.7	0.0	0.7	2.6	1.0
G-Protein Coupled Receptor Signaling	2.7	0.9	0.7	1.0	5.6
Estrogen Biosynthesis	0.3	0.0	0.0	0.0	6.9
Androgen Biosynthesis	1.2	0.0	0.3	0.0	4.1

Figure 4 Canonical pathway analysis, Ingenuity pathway analysis, excluding genes co-expressed in more than four tissues, displaying the −log(P-value) of the highest scoring pathways for each tissue. Shading indicates the significance levels visually: black, P < 0.001; dark grey, P < 0.01; light grey, P < 0.05.

similarity to mouse AVE markers and parietal endoderm/hypoblast.
- Cattle PH expression most resembles mouse visceral endoderm/hypoblast genes but notably shows little similarity to mouse parietal endoderm/hypoblast.
- Cattle TB shows some similarity (P < 0.05) only to genes expressed in mouse ectoplacental cone trophoblast tissue.

The five cattle tissues were also compared with lineage-specific cattle embryo datasets. Two published gene expression lists (Nagatomo *et al.*, 2013; Ozawa *et al.*, 2012) of cattle day 8 ICM (embryonic disc precursor) and trophectoderm were compared with the day 15 tissues (Fig. 3). As expected, all four ICM-derived tissues correlated well with the cattle ICM gene sets but not with the day 8 TE, whereas the converse was true for the trophoblastic tissues.

Pathway analyses

We next analysed the differentially expressed genes using Ingenuity pathway analysis (FPKM > 1, excluding common genes). The Stage 4 embryonic disc and its developmental derivatives, Stage 5 EmE and MEH, all scored highest for two categories of pathway (Fig. 4). One involves WNT signalling including both the canonical (β-CATENIN dependent) and non-canonical WNT/PCP (planar cell polarity) pathways. The other category is based on embryonic stem (ES) cell networks. MEH and PH tissues scored for cardiogenesis. Among the top hits for PH were PAK and actin cytoskeleton signalling. These are related as PAK mediates actin cytoskeletal rearrangements. TB scored highly for G-protein coupled receptor signalling and steroidogenic pathways with this tissue expressing all genes required for ADHE (dehydroepiandrosterone) to 5α-dihydro-testosterone or to estradiol-17β conversion.
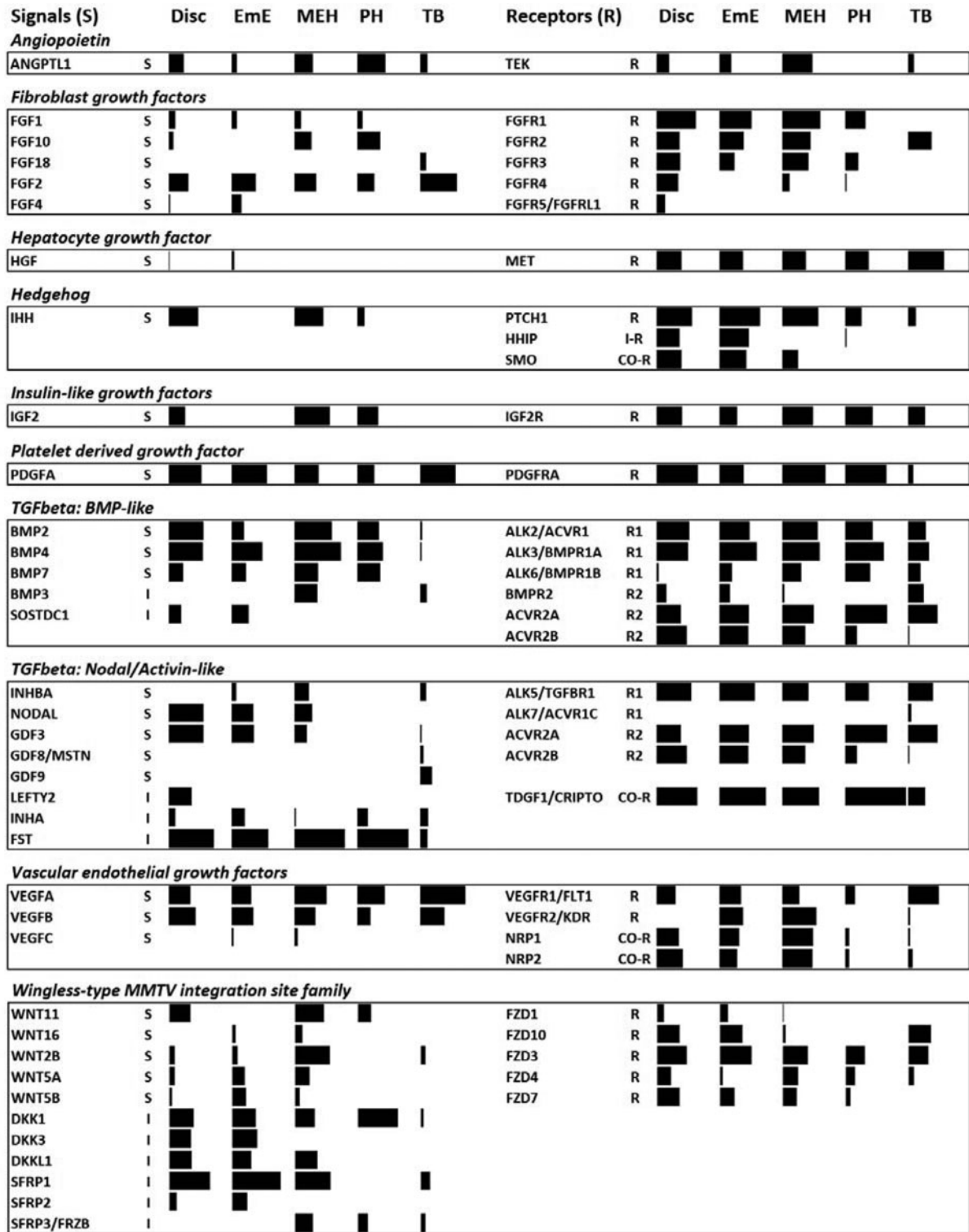
Figure 5 Expression levels of genes coding for secreted signalling factors (S), inhibitors (I), receptors (R) and co-receptors (CO-R) in embryonic tissues. The size of the black bars is proportional to the log of the expression level.

Signalling pathways were analysed in terms of receptor and ligand transcription, using all expressed genes and a curated list (Fig. S1) of 131 growth factors/cytokines and their 69 receptors/receptor co-factors derived from Ingenuity and KEGG databases. All ligand families, for which at least one signal and matching receptor was expressed, are depicted in Fig. 5. ANGIOPOIETIN-LIKE 1 is produced in large quantities by PH, though this tissue has no receptor for it, suggesting it acts on the adjacent TB tissue, which does express TEK. Of the growth factors that predominantly act through the RAS-RAF-Classical MAPK pathway, the ERBB (EGF) family was not detected. However, FGFs and PDGFs were found to be well represented. FGF2 is widely expressed at high levels, with hypoblast-containing tissues additionally expressing FGF10, and the EmE co-expressing FGF4. All tissues expressed a range of FGF receptors, except TB which only expressed FGFR2. PDGFA and its receptor were expressed in all tissues, albeit at highly variable levels with hypoblast-containing tissues (PH, MEH) containing abundant receptors, while the overlying epithelia (TB and EmE, respectively) expressing the most ligand, suggesting a paracrine interaction. VEGFA and B, which act via numerous intracellular pathways, were ubiquitously expressed, with the VEGFA receptor transcribed at the highest level in TB, whereas the B receptor and NRP co-receptors were exclusive to the EmE and MEH tissues. INSULIN-like signalling (IGF2) emanated predominantly from hypoblast-containing tissue, while receptors were ubiquitous. INDIAN HEDGEHOG was transcribed in the Stage 4 disc and Stage 5 MEH, with abundant receptor and co-receptors in disc, MEH and EmE, although disc and EmE also expressed high amounts of the inhibitory membrane protein HHIP. The BMP-branch of TGFβ signalling was well represented via BMP2, 4 and 7 expression in all tissues except TB, and ubiquitous expression of the receptors (Type 1: ALK2, ALK3, Type 2: ACVR2A). Few of the large array of BMP inhibitors were expressed. Of the TGFβ/NODAL/ACTIVIN-like ligands, TGFβ ligands were detected at less than 2 FPKM (not shown in Fig. 5), however, NODAL and GDF3 were robustly transcribed at Stage 4 and at Stage 5 in the EmE and MEH. The widespread and extensive transcription of the ACTIVIN inhibitor FOLLISTATIN would suggest that the modest amount of INHBA (ACTIVIN A subunit) made in MEH would have little effect. Curiously, the NODAL/GDF3 type 1 receptors ALK4 and ALK7 were absent in all tissues, whereas the TGFβ-specific ALK5 receptor was detected, as was the NODAL co-receptor CRIPTO. Lastly, WNT signalling, in concurrence with the pathway analyses, was prominent in the embryonic disc-related tissues (disc/EmE/MEH), while the receptor FRIZZLED-3

was expressed in all tissues at high levels. The main ligands were WNT11 (disc, EmE), WNT2B (MEH) and WNT5A and B (EmE, MEH). Notably, WNT inhibitors are also expressed at very high levels, in particular SFRP1 in the disc-related tissues, and DKK1 in PH.

Discussion

The pre-gastrulation Stage 4 embryonic disc

The Stage 4 disc is a heterogeneous structure, characterised by a 2-cell layered epithelium that is the embryonic ectoderm (EmE) and the visceral hypoblast layer beneath it. Both are derived from the ICM and the transcriptome of the disc showed the greatest resemblance of all five tissues to ICM gene sets. One important developmental event occurring as embryos transit from Stage 3 to Stage 4 is the expansion of the anterior visceral hypoblast (AVH) signalling centre and indeed the mouse AVE-specific markers LEFTY2, GSC, SFRP1 and HHEX were detected in the Stage 4 embryonic disc. CER1, a cattle AVH marker detectable by *in situ* hybridization (van Leeuwen *et al.*, 2015), lay below our cut-off, possibly because of a combination of low expression and a limited expression domain. In terms of signalling pathways, at this stage NODAL becomes progressively restricted to the posterior end of the EmE, where it induces the process of gastrulation (van Leeuwen *et al.*, 2015). We noted the disc to express the highest levels of NODAL, as well as GDF3, which can also signal via the NODAL pathway (Andersson *et al.*, 2007). Surprisingly though, while type 2 NODAL/GDF3 receptors and the essential NODAL signalling cofactor CRIPTO were robustly expressed, neither of the required type 1 receptors (ALK4, ALK7) known to mediate NODAL signalling in mouse embryos (Moustakas & Heldin, 2009) could be detected. Potentially the strongly expressed ALK5 receptor, known to mediate signalling for other members of this branch of TGFβ ligands (such as TGFβ1–3, GDF1, 3, 8, 9) (Moustakas & Heldin, 2009), is used at these cattle embryonic stages to transmit NODAL signalling. Alternatively, in cattle, GDF3 could be mediating the effects attributed to NODAL in the mouse. This issue merits further investigation. WNT signalling was evidenced by *WNT11* and receptors *FZD3*, *4*, *7* and *10* expression. Significantly, WNT11 signals via the PCP non-canonical pathway and this pathway has been linked in amniotes to medio-lateral cell intercalations in the embryonic ectoderm preceding and during gastrulation (Voiculescu *et al.*, 2007). FGF signalling is represented by FGF2 and transcription of all known FGF receptors. The exclusive expression of FGF2 differs from mouse embryos, which do not

express FGF2 until mid-gastrulation stages (Wordinger *et al.*, 1994; Taniguchi *et al.*, 1998), but express the closely related FGF4 and FGF8 instead (Niswander & Martin, 1992; Crossley & Martin, 1995).

The Stage 5 extraembryonic ectoderm (EmE)

The Stage 5 EmE and Stage 4 disc are remarkably similar in terms of: (i) their transcriptomes, uniquely sharing 389 genes; (ii) their transcriptomes plot closely together upon PCA analysis; (iii) these tissues sharing the same top five canonical pathways; and (iv) scoring similarly highly in comparisons with the mouse epiblast/embryonic ectoderm gene set. The Stage 5 EmE as well as Stage 4 disc expressed all three master regulators of stemness/pluripotency, namely *POU5F1* (*OCT4*), *SOX2* and *NANOG* (Boyer *et al.*, 2005; Wang *et al.*, 2012) as well as *KLF4*, *OTX2*, *PRDM14*, *SALL4*, *STAT3* and *ZIC3* (Tsubooka *et al.*, 2009; Acampora *et al.*, 2013; Dunn *et al.*, 2014). The function of the Oct4−SOX2−NANOG (OSN) network is to keep cells in an undifferentiated state primed for differentiation and thus the continued expression of the OSN network is likely to explain the overall similarity of gene expression in the EmE tissues of Stages 4 and 5. Interestingly, these tissues also displayed a high similarity to the list of mouse primordial germ cell (PGC) markers. In mouse embryos, PGC are specified in the embryonic ectoderm from embryonic day 6.25, just before gastrulation starts (Magnúsdóttir *et al.*, 2012). While the first PGC-specifying gene, *PRDM1* (*BLIMP1*) and the PGC marker *DDX4* are transcribed only early on, at Stage 4, the downstream cascade represented by *PRDM14*, which is essential for PGC development, *TFAP2C*, *DND1*, and the requisite pluripotency OSN triumvirate (Youngren *et al.*, 2005; Yamaji *et al.*, 2008; Magnúsdóttir *et al.*, 2013), are all expressed at both stages. We conclude that in cattle, PGCs originate around Stage 4 and are found in the embryonic ectoderm layer at Stage 5, when gastrulation starts.

In mice, gastrulation is preceded by NODAL signals switching on canonical WNT signalling in the embryonic ectoderm and BMP signals in the adjacent trophoblast, with all three signals then required for inducing prospective endoderm and mesoderm [reviewed in (Arnold & Robertson, 2009)]. NODAL/GDF3 and WNT signal/receptor transcription was also seen in the cattle embryonic ectoderm, however, unlike the mouse, BMP2/4/7 ligands were not expressed in the trophoblast but induced in the EmE itself, as well as in the subjacent layer of hypoblast/mesendoderm (the MEH). This situation makes sense in that, in cattle, no trophoblast tissue overlies the EmE at these stages, due to the different morphology of the cattle and mouse early gastrula.

A second difference lies in the specific WNT ligand expressed: mice require WNT3 for gastrulation (Liu *et al.*, 1999), but in cattle WNT5B is expressed instead. Molecularly, NODAL/WNT/BMP signalling switches on three key genes that drive mesendoderm generation in vertebrates, namely *EOMESODERMIN*, *BRACHYURY* and *MIXL1* (Arnold *et al.*, 2000; Hart *et al.*, 2002; Hart *et al.*, 2005; Robertson, 2014). The cattle homologues are all expressed in the Stage 5 embryonic ectoderm (Table S1). In mice, prospective mesendodermal cells in the embryonic ectoderm are induced to undergo a epithelial−mesenchymal transition and to migrate out of this layer under the influence of FGF signalling, as shown by FGF8 (with concomitant loss of FGF4 expression) and FGFR1 knock-outs (Sun *et al.*, 1999; Brewer *et al.*, 2015). Notably, FGF8 expression was not detected in cattle embryos, however the ubiquitous FGF2 transcription was boosted in Stage 5 EmE by FGF4 expression. As FGF2/4/8 all activate the same receptor isoforms (Ornitz *et al.*, 1996), the change in the cattle versus mouse transcriptional networks may be without phenotypic consequence.

The lower layer of the Stage 5 embryonic disc

Gene expression comparisons of the MEH with the mouse lists indicated the expression of node and primitive streak markers pointing to nascent mesendoderm formation. Interestingly the ingressing cells exhibited mainly extraembryonic mesoderm and endoderm characteristics, whereas embryonic mesoderm markers were not expressed. We conclude that in cattle, cells giving rise to definitive endoderm and mesodermal cells of extraembryonic fate are the first to migrate out of the EmE. Extraembryonic mesoderm cells are those that subsequently line the trophoblast, yolk sac and amnion and presumably also give rise to the allantois (Maddox-Hyttel *et al.*, 2003; Vejlsted *et al.*, 2006).

In mice the (embryonic) visceral hypoblast/endoderm lines the EmE (Kaufman, 1995). In this species the cup-shaped EmE abuts along its rim a distinct type of proliferative trophoblast, termed the extraembryonic ectoderm (ExE). At the implantation end of the egg cylinder the ExE then merges into the ectoplacental cone (EPC) and the rest of the mural trophoblast. The hypoblast that lines the ExE is the extraembryonic visceral hypoblast and that covering the EPC and rest of the mural trophoblast is the parietal hypoblast. This distinction between embryonic and extraembryonic visceral hypoblast cannot be made in cattle embryos based on morphological criteria, as no anatomical homologue to the ExE exists in this species. Similarly, the MEH gene expression data comparisons with the mouse tissues

allow no molecular distinction to be made between these two types of visceral hypoblast tissue in cattle.

In comparison with the EmE, the MEH layer exhibited a distinctly different signalling transcriptome:

(i). TGFβ signalling was shifted from a NODAL-like to a BMP-like dominant program. This is likely related to the formation of the extraembryonic mesoderm as BMPs have been shown to be essential for the development of this tissue (Zhang & Bradley, 1996).

(ii). WNT ligands were transcribed at greater levels with the appearance of WNT11 and WNT2B as well as WNT5A transcription. The overall much lower levels of receptors (FRIZZLED 1 and 10 were switched off) points to a MEH-derived WNT role predominantly in the overlying EmE. The high levels of WNT2A in the MEH may aid in canonical WNT signalling in the EmE as previously discussed, whereas WNT5A and WNT11 have been associated with planar cell polarity (PCP) mediated convergence extension movements required, at this stage, for the lengthening of the primitive streak (Andre *et al.*, 2015).

(iii). The appearance of FGF10 in MEH (and PH) may be cattle-specific as FGF10 is seen in mouse embryos only at late gastrulation stages (Tagashira *et al.*, 1997).

(iv). HEDGEHOG signalling ligands and receptors (*IHH*, *PTCH1*, *SMO*) were detected in the EmE/VH tissues of the Stage 4 disc and this signalling is continued at Stage 5 with the signal, INDIAN HEDGEHOG (IHH), being exclusively transcribed in the visceral hypoblast-containing MEH layer. During mouse embryogenesis, IHH is expressed only in the VH, but required for the differentiation of the adjacent EmE into neuroectoderm as gastrulation commences (Maye *et al.*, 2004). The expression of IHH receptor and co-receptor (PTCH1 and SMO) in the EmE (*SMO* is transcribed at three-fold lower levels in the MEH) supports a similar vertical signalling role for IHH in cattle EmE specification.

(v). Similarly, IGF2 is expressed in MEH, but not EmE, whereas the receptor is ubiquitous.

Parietal hypoblast

The cattle parietal hypoblast underlying the trophoblast is destined, together with a lining of extraembryonic mesoderm, to form the yolk sac (Betteridge & Flechon, 1988). The overlap with the mouse parietal hypoblast marker list was not significant. Instead a high significance was seen with mouse embryonic

and extraembryonic visceral hypoblast, suggesting that the differentiation of hypoblast into the visceral and parietal lineages is dissimilar in mice and cattle. Pathway analyses gave few clues as to the function of this tissue with relatively low significant hits of a more general nature, including two matches for pathways involving the actin cytoskeleton.

The PH transcribes few growth factors and a more limited range of receptors than the previously discussed tissues. In particular NODAL-like and WNT signals are not transcribed and receptors for FGF, VEGF, HEDGEHOG, WNT and ANGEIOPOIETIN signalling are absent or transcribed at low levels. However, PDGF receptor A is expressed at very high levels and the overlying TB produces the ligand at very high levels. Indeed in mouse embryos roles for PDGFRA in the expansion of the hypoblast and formation of the yolk sac has been shown (Ogura *et al.*, 1998; Artus *et al.*, 2010). This role is likely to be conserved in cattle with the likely source being trophoblastic.

The high expression of ANGIOPOIETIN-LIKE-1, but not its receptor, may relate to the paracrine induction of blood vessels in the extraembryonic mesoderm, which will line this layer at later stages.

Trophoblast

The Stage 5 trophoblast exhibited the most unique transcriptome of those investigated, as seen in the principal component analysis and the large set of uniquely expressed genes. This uniqueness ties in with the fact that the trophoblast is the first lineage to be specified and that by day 14, TB is committed to its fate (Berg *et al.*, 2011). This situation is corroborated by the switching on of steroidogenic enzyme transcription (pathway analyses), characteristic of steroid-hormone producing mature trophoblast. Unexpectedly, the mouse trophoblast-specific gene lists aligned slightly more significantly to the cattle EmE than TB. The mouse gene lists were assembled from genes expressed either in the extraembryonic ectoderm (ExE) or the ectoplacental cone (EPC). The ExE, from which mouse trophoblast stem cells can be derived, harbours predominantly undifferentiated trophoblast cells some of which will give rise to syncytiotrophoblast cells, while the EPC contains more differentiated cells, destined to become either spongiotrophoblast or various types of secondary giant cells (Pfeffer & Pearton, 2012). Cattle do not appear to contain cells equivalent to syncytio- or spongiotrophoblast thus explaining the low concordance with the mouse trophoblast lists. More fundamentally, the trophoblast differences highlight that this tissue, which gives rise to the placenta, is evolutionarily speaking relatively new, its origin lying near the start of the divergence of eutherian mammals. Different species of mammals

have elaborated on the requirements of gestation in radically different ways (such as the cattle minimally invasive synepitheliochorial versus the mouse invasive hemochorial modes of placentation), requiring large adaptive changes in the trophoblast which would be reflected in distinct transcriptomes.

In spite of these differences, two key trophoblast aspects appear to have been at least partly conserved. The first is lineage specification. In mice the trophoblast lineage specification and determination network involves the key genes *Cdx2, Gata3, Tfap2a, Tfap2c, Elf5, Eomes* and *Ets2* with *Ascl2* appearing in slightly more differentiated cells (Pfeffer & Pearton, 2012). Except for *Eomes*, these genes were also detected in Stage 5 TB. The absence of *EOMES* from cattle TB has been noted previously using real-time PCR (Smith *et al.*, 2010). The second commonality involves FGF signalling, which appears to be involved in both species although with a distinct variation in signal source. Mouse proliferative trophoblast and trophoblast stem cells exhibit a requirement for FGF signalling believed to emanate *in vivo* predominantly from the mouse EmE in the form of FGF4 (Tanaka *et al.*, 1998). We found here that Stage 5 TB contains FGFR2 and synthesises FGF2 itself. Further FGF signalling may be delivered in a paracrine fashion in the form of FGF10 transcribed in the subjacent PH. Due to the different topology of the mouse and cattle conceptuses, cattle embryos cannot rely on the EmE as a FGF source, because unlike in the mouse, most of the cattle trophoblast is simply physically to distant from this EmE. Hence an autocrine production of this signal and/or a supply from the hypoblast may be adaptations to meet a conserved TB requirement for FGF signalling.

This analysis of the transcriptome of all four major tissues of the same embryo at a single moment of developmental time allowed unique insights into the different events occurring at the start of gastrulation. While focussing on tissues of a single embryo ensures consistency in terms of developmental stage, it does not address issues of consistency of expression across similarly staged embryos. Such expression may vary for some genes such as those exhibiting oscillatory behaviour (Phillips *et al.*, 2016). As more studies of all tissues of individual embryo transcriptomes are analysed a full and detailed transcriptional atlas will be able to be mapped out, paving the way for assembling the gene regulatory networks that need to be understood so as to alleviate early embryo mortality.

Acknowledgements

Supporting information

Supporting information is available for this article online at the publisher's website.
Figure S1 and Table S1

Supplementary material

To view supplementary material for this article, please visit https://doi.org/10.1017/S0967199417000090

References

Acampora, D., Di Giovannantonio, L.G. & Simeone, A. (2013). Otx2 is an intrinsic determinant of the embryonic stem cell state and is required for transition to a stable epiblast stem cell condition. *Development* **140**, 43–55.

Andersson, O., Bertolino, P. & Ibanez, C.F. (2007). Distinct and cooperative roles of mammalian Vg1 homologs GDF1 and GDF3 during early embryonic development. *Dev. Biol.* **311**, 500–11.

Andre, P., Song, H., Kim, W., Kispert, A. & Yang, Y. (2015). Wnt5a and Wnt11 regulate mammalian anterior-posterior axis elongation. *Development* **142**, 1516–27.

Arnold, S.J. & Robertson, E.J. (2009). Making a commitment: cell lineage allocation and axis patterning in the early mouse embryo. *Nat. Rev. Mol. Cell Biol.* **10**, 91–103.

Arnold, S.J., Stappert, J., Bauer, A., Kispert, A., Herrmann, B.G. & Kemler, R. (2000). Brachyury is a target gene of the Wnt/beta-catenin signalling pathway. *Mech. Dev.* **91**, 249–58.

Artus, J., Panthier, J.J. & Hadjantonakis, A.K. (2010). A role for PDGF signalling in expansion of the extraembryonic endoderm lineage of the mouse blastocyst. *Development* **137**, 3361–72.

Ayalon, N. (1978). A review of embryonic mortality in cattle. *J. Reprod. Fertil.* **54**, 483–93.

Berg, D.K., Smith, C.S., Pearton, D.J., Wells, D.N., Broadhurst, R., Donnison, M. & Pfeffer, P.L. (2011). Trophectoderm lineage determination in cattle. *Dev. Cell.* **20**, 244–55.

Berg, D.K., van Leeuwen, J., Beaumont, S., Berg, M. & Pfeffer, P.L. (2010). Embryo loss in cattle between days 7 and 16 of pregnancy. *Theriogenology* **73**, 250–60.

Betteridge, K.J. & Flechon, J.E. (1988). The anatomy and physiology of pre-attachment bovine embryos. *Theriogenology* **29**, 155–87.

Boyer, L.A., Lee, T.I., Cole, M.F., Johnstone, S.E., Levine, S.S., Zucker, J.P., Guenther, M.G., Kumar, R.M., Murray, H.L., Jenner, R.G., Gifford, D.K., Melton, D.A., Jaenisch, R. & Young, R.A. (2005). Core transcriptional regulatory circuitry in human embryonic stem cells. *Cell* **122**, 947–56.

Brewer, J.R., Molotkov, A., Mazot, P., Hoch, R.V. & Soriano, P. (2015). Fgfr1 regulates development through the

combinatorial use of signalling proteins. *Genes Dev.* **29**, 1863–74.

Brown, K., Legros, S., Artus, J., Doss, M.X., Khanin, R., Hadjantonakis, A.K. & Foley, A. (2010). A comparative analysis of extraembryonic endoderm cell lines. *PLoS One* **5**, e12016.

Crossley, P.H. & Martin, G.R. (1995). The mouse Fgf8 gene encodes a family of polypeptides and is expressed in regions that direct outgrowth and patterning in the developing embryo. *Development* **121**, 439–51.

Diskin, M.G., Parr, M.H. & Morris, D.G. (2011). Embryo death in cattle: an update. *Reprod. Fertil. Dev.* **24**, 244–51.

Dodt, M., Roehr, J.T., Ahmed, R. & Dieterich, C. (2012). FLEXBAR − flexible barcode and adapter processing for next-generation sequencing platforms. *Biology (Basel)* **1**, 895–905.

Dunn, S.J., Martello, G., Yordanov, B., Emmott, S. & Smith, A.G. (2014). Defining an essential transcription factor program for naive pluripotency. *Science* **344**, 1156–60.

Ewen, K.A. & Koopman, P. (2010). Mouse germ cell development: From specification to sex determination. *Mol. Cell. Endocrinol.* **323**, 76–93.

Familari, M. (2006). Characteristics of the endoderm: embryonic and extraembryonic in mouse. *Sci. World J.* **6**, 1815–27.

Hart, A.H., Hartley, L., Sourris, K., Stadler, E.S., Li, R., Stanley, E.G., Tam, P.P., Elefanty, A.G. & Robb, L. (2002). Mixl1 is required for axial mesendoderm morphogenesis and patterning in the murine embryo. *Development* **129**, 3597–608.

Hart, A.H., Willson, T.A., Wong, M., Parker, K. & Robb, L. (2005). Transcriptional regulation of the homeobox gene Mixl1 by TGF-beta and FoxH1. *Biochem. Biophys. Res. Commun.* **333**, 1361–9.

Kaufman, M.H. (1995). *The Atlas of Mouse Development*, Academic Press, London.

Li, H. & Durbin, R. (2009). Fast and accurate short read alignment with Burrows−Wheeler transform. *Bioinformatics* **25**, 1754–60.

Liu, P., Wakamiya, M., Shea, M.J., Albrecht, U., Behringer, R.R. & Bradley, A. (1999). Requirement for Wnt3 in vertebrate axis formation. *Nat. Genet.* **22**, 361–5.

Lu, C.C., Brennan, J. & Robertson, E.J. (2001). From fertilization to gastrulation: axis formation in the mouse embryo. *Curr Opin Genet Dev.* **11**, 384–92.

Maddox-Hyttel, P., Alexopoulos, N.I., Vajta, G., Lewis, I., Rogers, P., Cann, L., Callesen, H., Tveden-Nyborg, P. & Trounson, A. (2003). Immunohistochemical and ultrastructural characterization of the initial post-hatching development of bovine embryos. *Reproduction* **125**, 607–23.

Magnúsdóttir, E., Dietmann, S., Murakami, K., Günesdogan, U., Tang, F., Bao, S., Diamanti, E., Lao, K., Gottgens, B. & Azim Surani, M. (2013). A tripartite transcription factor network regulates primordial germ cell specification in mice. *Nat. Cell Biol.* **15**, 905–15.

Magnúsdóttir, E., Gillich, A., Grabole, N. & Surani, M.A. (2012). Combinatorial control of cell fate and reprogramming in the mammalian germline. *Curr. Opin. Genet. Dev.* **22**, 466–74.

Mamo, S., Mehta, J.P., McGettigan, P., Fair, T., Spencer, T.E., Bazer, F.W. & Lonergan, P. (2011). RNA sequencing reveals novel gene clusters in bovine conceptuses associated with maternal recognition of pregnancy and implantation. *Biol. Reprod.* **85**, 1143–51.

Maye, P., Becker, S., Siemen, H., Thorne, J., Byrd, N., Carpentino, J. & Grabel, L. (2004). Hedgehog signalling is required for the differentiation of ES cells into neurectoderm. *Dev. Biol.* **265**, 276–90.

Mortazavi, A., Williams, B.A., McCue, K., Schaeffer, L. & Wold, B. (2008). Mapping and quantifying mammalian transcriptomes by RNA-seq. *Nat. Method.* **5**, 621–8.

Moustakas, A. & Heldin, C.H. (2009). The regulation of TGFbeta signal transduction. *Development* **136**, 3699–714.

Nagatomo, H., Kagawa, S., Kishi, Y., Takuma, T., Sada, A., Yamanaka, K., Abe, Y., Wada, Y., Takahashi, M., Kono, T. & Kawahara, M. (2013). Transcriptional wiring for establishing cell lineage specification at the blastocyst stage in cattle. *Biol. Reprod.* **88**, 158.

Niswander, L. & Martin, G.R. (1992). Fgf-4 expression during gastrulation, myogenesis, limb and tooth development in the mouse. *Development* **114**, 755–68.

Ogura, Y., Takakura, N., Yoshida, H. & Nishikawa, S.I. (1998). Essential role of platelet-derived growth factor receptor alpha in the development of the intraplacental yolk sac/sinus of Duval in mouse placenta. *Biol. Reprod.* **58**, 65–72.

Ornitz, D.M., Xu, J., Colvin, J.S., McEwen, D.G., MacArthur, C.A., Coulier, F., Gao, G. & Goldfarb, M. (1996). Receptor specificity of the fibroblast growth factor family. *J. Biol. Chem.* **271**, 15292–7.

Ozawa, M., Sakatani, M., Yao, J., Shanker, S., Yu, F., Yamashita, R., Wakabayashi, S., Nakai, K., Dobbs, K.B., Sudano, M.J., Farmerie, W.G. & Hansen, P.J. (2012). Global gene expression of the inner cell mass and trophectoderm of the bovine blastocyst. *BMC Dev. Biol.* **12**, 33.

Pearton, D.J., Smith, C.S., Redgate, E., van Leeuwen, J., Donnison, M. & Pfeffer, P.L. (2014). Elf5 counteracts precocious trophoblast differentiation by maintaining Sox2 and 3 and inhibiting Hand1 expression. *Dev. Biol.* **392**, 344–57.

Pfeffer, P.L. (2014). Lineage commitment in the mammalian preimplantation embryo. In *Reproduction in Domestic Ruminants* vol. 8 (eds J. Juengel, A. Miyamoto, & R. Webb) pp. 89–103. Context, Obihiro, Japan.

Pfeffer, P.L. & Pearton, D.J. (2012). Trophoblast development. *Reproduction* **143**, 231–46.

Phillips, N.E., Manning, C.S., Pettini, T., Biga, V., Marinopoulou, E., Stanley, P., Boyd, J., Bagnall, J., Paszek, P., Spiller, D.G., White, M.R.H., Goodfellow, M., Galla, T., Rattray, M. & Papalopulu, N. (2016). Stochasticity in the miR-9/Hes1 oscillatory network can account for clonal heterogeneity in the timing of differentiation. *eLife* **5**, e16118.

R Core Team (2014). *R: a language and environment for statistical computing*. R Foundation for Statistical Computing, Vienna, Austria.

Richardson, L., Venkataraman, S., Stevenson, P., Yang, Y., Moss, J., Graham, L., Burton, N., Hill, B., Rao, J., Baldock, R.A. & Armit, C. (2014). EMAGE mouse embryo spatial gene expression database: 2014 update. *Nucl. Acid Res.* **42**, D835–44.

Rielland, M., Hue, I., Renard, J.P. & Alice, J. (2008). Trophoblast stem cell derivation, cross-species comparison and use of nuclear transfer: new tools to study trophoblast growth and differentiation. *Dev. Biol.* **322**, 1–10.

Roberts, R.M. & Fisher, S.J. (2011). Trophoblast stem cells. *Biol. Reprod.* **84**, 412–21.

Robertson, E.J. (2014). Dose-dependent Nodal/Smad signals pattern the early mouse embryo. *Semin. Cell. Dev. Biol.* **32**, 73–9.

Robinson, M.D., McCarthy, D.J. & Smyth, G.K. (2010). edgeR: a Bioconductor package for differential expression analysis of digital gene expression data. *Bioinformatics* **26**, 139–40.

Sartori, R., Bastos, M.R. & Wiltbank, M.C. (2010). Factors affecting fertilization and early embryo quality in single- and superovulated dairy cattle. *Reprod. Fertil. Dev.* **22**, 151–8.

Smith, C., Berg, D., Beaumont, S., Standley, N.T., Wells, D.N. & Pfeffer, P.L. (2007). Simultaneous gene quantitation of multiple genes in individual bovine nuclear transfer blastocysts. *Reproduction* **133**, 231–42.

Smith, C.S., Berg, D.K., Berg, M. & Pfeffer, P.L. (2010). Nuclear transfer-specific defects are not apparent during the second week of embryogenesis in cattle. *Cell Reprogram.* **12**, 699–707.

Sun, X., Meyers, E.N., Lewandoski, M. & Martin, G.R. (1999). Targeted disruption of Fgf8 causes failure of cell migration in the gastrulating mouse embryo. *Genes Dev.* **13**, 1834–46.

Tagashira, S., Harada, H., Katsumata, T., Itoh, N. & Nakatsuka, M. (1997). Cloning of mouse FGF10 and up-regulation of its gene expression during wound healing. *Gene* **197**, 399–404.

Tanaka, S., Kunath, T., Hadjantonakis, A.K., Nagy, A. & Rossant, J. (1998). Promotion of trophoblast stem cell proliferation by FGF4. *Science* **282**, 2072–5.

Taniguchi, F., Harada, T., Yoshida, S., Iwabe, T., Onohara, Y., Tanikawa, M. & Terakawa, N. (1998). Paracrine effects of bFGF and KGF on the process of mouse blastocyst implantation. *Mol. Reprod. Dev.* **50**, 54–62.

Trapnell, C., Pachter, L. & Salzberg, S.L. (2009). TopHat: discovering splice junctions with RNA-seq. *Bioinformatics* **25**, 1105–11.

Tsubooka, N., Ichisaka, T., Okita, K., Takahashi, K., Nakagawa, M. & Yamanaka, S. (2009). Roles of Sall4 in the generation of pluripotent stem cells from blastocysts and fibroblasts. *Genes Cells* **14**, 683–94.

van Leeuwen, J., Berg, D.K. & Pfeffer, P.L. (2015). Morphological and gene expression changes in cattle embryos from hatched blastocyst to early gastrulation stages after transfer of *in vitro* produced embryos. *PLoS One* **10**, e0129787.

Vejlsted, M., Du, Y., Vajta, G. & Maddox-Hyttel, P. (2006). Post-hatching development of the porcine and bovine embryo—defining criteria for expected development *in vivo* and *in vitro*. *Theriogenology* **65**, 153–65.

Voiculescu, O., Bertocchini, F., Wolpert, L., Keller, R.E. & Stern, C.D. (2007). The amniote primitive streak is defined by epithelial cell intercalation before gastrulation. *Nature* **449**, 1049–52.

Wang, Z., Oron, E., Nelson, B., Razis, S. & Ivanova, N. (2012). Distinct lineage specification roles for NANOG, OCT4, and SOX2 in human embryonic stem cells. *Cell. Stem Cell* **10**, 440–54.

Wooding, F.B. (1992). Current topic: the synepitheliochorial placenta of ruminants: binucleate cell fusions and hormone production. *Placenta* **13**, 101–13.

Wordinger, R.J., Smith, K.J., Bell, C. & Chang, I.F. (1994). The immunolocalization of basic fibroblast growth factor in the mouse uterus during the initial stages of embryo implantation. *Growth Factors* **11**, 175–86.

Yamaji, M., Seki, Y., Kurimoto, K., Yabuta, Y., Yuasa, M., Shigeta, M., Yamanaka, K., Ohinata, Y. & Saitou, M. (2008). Critical function of Prdm14 for the establishment of the germ cell lineage in mice. *Nat. Genet.* **40**, 1016–22.

Yanai, I., Benjamin, H., Shmoish, M., Chalifa-Caspi, V., Shklar, M., Ophir, R., Bar-Even, A., Horn-Saban, S., Safran, M., Domany, E., Lancet, D. & Shmueli, O. (2005). Genome-wide midrange transcription profiles reveal expression level relationships in human tissue specification. *Bioinformatics* **21**, 650–9.

Youngren, K.K., Coveney, D., Peng, X., Bhattacharya, C., Schmidt, L.S., Nickerson, M.L., Lamb, B.T., Deng, J.M., Behringer, R.R., Capel, B., Rubin, E.M., Nadeau, J.H. & Matin, A. (2005). The Ter mutation in the dead end gene causes germ cell loss and testicular germ cell tumours. *Nature* **435**, 360–4.

Zhang, H. & Bradley, A. (1996). Mice deficient for BMP2 are nonviable and have defects in amnion/chorion and cardiac development. *Development* **122**, 2977–86.